E3-2008-138

M. Balasoiu[1,3], E. M. Anitas[1,2], I. Bica[1,2], V. A. Osipov[1],
O. L. Orelovich[1], D. Savu[2], S. Savu[2], R. Erhan[1,3], A. I. Kuklin[1]

SANS OF INTERACTING MAGNETIC MICRO-SIZED Fe PARTICLES IN A STOMAFLEX CREME POLYMER MATRIX

Submitted to «Journal of Optoelectronics and Advanced Materials — RC»

[1]Joint Institute for Nuclear Research, Dubna, Russia
[2]The West University of Timisoara, Timisoara, Romania
[3]Horia Hulubei National Institute of Physics and Nuclear Engineering, Bucharest, Romania

Балашою М. и др. E3-2008-138
Малоугловое рассеяние нейтронов
на взаимодействующих частицах железа микронного размера
в полимерной матрице Stomaflex

Рассматриваются результаты малоуглового нейтронного рассеяния магнитных эластомеров, поляризованных без поля и при наличии магнитного поля, при 25, 50 и 75 % массовой концентрации частиц Fe среднего радиуса 2,09 мкм в полимерной матрице Stomaflex. При полимеризации было использовано магнитное поле 156,5 мТл. Кривые интенсивности малоуглового нейтронного рассеяния имеют сходное поведение для всех концентраций, что свидетельствует о том, что для данных размеров частиц и поля 156,5 мТл микроструктура магнитных эластомеров неизменна для диапазона q от 0,006 до 0,1 Å^{-1} и интенсивность рассеяния возрастает пропорционально массовой концентрации частиц Fe.

Работа выполнена в Лаборатории теоретической физики им. Н. Н. Боголюбова ОИЯИ.

Препринт Объединенного института ядерных исследований. Дубна, 2008

Balasoiu M. et al. E3-2008-138
SANS of Interacting Magnetic Micro-Sized Fe Particles in a Stomaflex
Creme Polymer Matrix

The investigations results obtained from small-angle neutron scattering on magnetic elastomers polymerized with and without magnetic field at 25, 50 and 75% mass concentration of Fe particles with a mean radius of 2.09 μm inside a Stomaflex creme polymer matrix have been reported. The magnetic field used in polymerization process is 156.5 mT. The profiles of the curves from SANS have a similar behavior for each concentration, showing that for these sizes of particles and polymerization process at 156.5 mT, the microstructure of magnetic elastomers is the same in the q-range of $0.006 - 0.1$ Å^{-1}, and scattering intensities increase proportionally with increasing the mass concentration of Fe particles.

The investigation has been performed at the Bogoliubov Laboratory of Theoretical Physics, JINR.

Preprint of the Joint Institute for Nuclear Research. Dubna, 2008

INTRODUCTION

Principal advantage of composite materials resides in the possibility of combining physical properties of the constituents to obtain new structural or functional properties. The scientific efforts in this field were therefore focused on the comprehension and optimization of the structural performances of these materials. Increased demand for high performance control design in combination with recent advances in condensed matter physics have produced a class of systems termed smart, intelligent or adaptive. Magnetic elastomers are a class of smart materials which consist of polymers with nano- and micro-sized particles, and show a great promise for many industrial and technological applications, due to the enhanced properties compared with classic materials. Therefore informations on the microstructure of such materials are very useful for understanding their behavior in different limiting conditions as required by industry and technology. The reinforcement of polymeric matrix with fine-particle metallic fillers to improve the physical properties (magnetic susceptibility, electrical conductivity, etc.) of polymeric materials [1] is widely used in industry.

A precise description of the microscopic structure from electron or atomic force microscopy techniques is often difficult to obtain. Scattering techniques [2,3] (neutrons, X-rays, light) are proved to be a very powerful tool for investigation the microstructure, organization and dynamics of matter. This is because the physical quantities, averaged over the whole sample (i.e., radius of gyration, specific surface), can be extracted with almost no approximation or model. Particularly, small-angle neutron scattering (SANS) [4, 5] is suitable for structural analysis and it is the method used in this paper to reveal the structure of Stomaflex creme polymer filled with Fe particles. The obtained information from the SANS curves serves a lot of purposes ranging from understanding the way in which particles are distributed in the polymer matrix till the possibility of controlling certain material properties. For magnetic elastomers the SANS is a result of the interactions between neutrons and atomic nuclei (nuclear scattering) on the one hand, and interactions between magnetic moments of neutrons and magnetic atoms (magnetic scattering) on the other hand.

In this paper the study was conducted to determine the effect of embedding of Fe micro-sized particles in a Stomaflex creme polymer matrix, polymerized in zero field and in magnetic field on the small-angle neutron scattering curve from magnetic elastomers.

1. EXPERIMENTAL

Magnetic elastomers systems analyzed here, obtained from reinforcement of spherical Fe particles [6] into a Stomaflex creme polymer matrix (Fig. 1 and Fig. 2), were prepared at the Faculty of Physics, The West University of Timisoara by Prof. I. Bica.

Two types of magnetic elastomers were analyzed: polymerized in zero field and polymerized in magnetic field. For each type there were three different mass concentrations investigated: 25, 50 and 75%, respectively. The magnetic field applied is $B = 156.5$ mT for each concentration. The polymer matrix consists of: a) Paste: alpha-omega polydimethylsiloxane — $[\mathrm{Si(CH_3)_2O}]_\mathrm{n}$, calcium carbonate — $\mathrm{CaCO_3}$, pigments, taste ingredients and b) Catalyst: dibutyltindilaureate, benzyl silicate, pigments.

Scanning electron microscopy images were obtained on Fe particles for determining the size distribution of the magnetic particles. They were analyzed using a MCID image analyzer software [7]. By processing these images, a distribution (Fig. 3) of the particles with the parameters: mean radius $R = 2.09$ μm, standard deviation $\sigma = 0.26$ μm, minimum radius $R_{\min} = 1.58$ μm and maximum radius $R_{\max} = 2.85$ μm were determined.

Small-angle neutron scattering experiments of nonpolarized neutrons were carried out at YUMO small-angle time-of-flight diffractometer [8, 9] at the IBR-2 pulsed reactor, JINR, Dubna, Russia. A two-detector system was used. The dif-

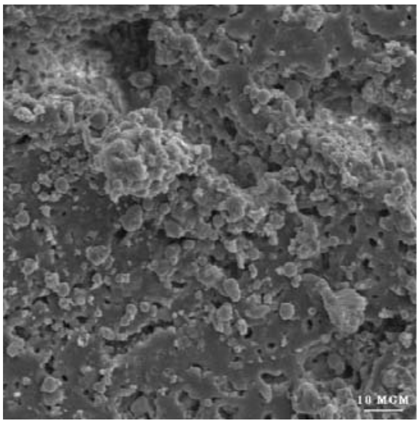

Fig. 1. Stomaflex creme + 25% Fe particles

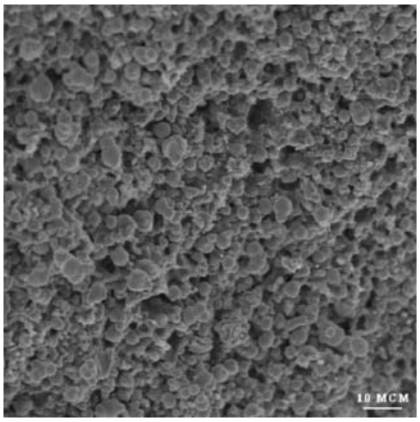

Fig. 2. Stomaflex creme + 75% Fe particles

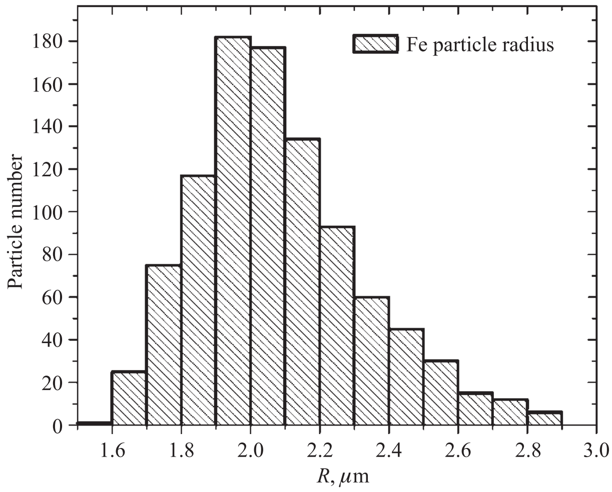

Fig. 3. Size distributions of Fe particles from EM images

ferential cross section per sample volume (scattering intensity) isotropic over the radial angle on the detector was obtained as a function of the module of momentum transfer, $q = (4\pi/\lambda)\sin(\theta/2)$, where λ is the incident neutron wavelength and θ is the scattering angle.

The neutron wavelengths within an interval of $0.05 - 0.5$ nm were used to obtain scattering curves (Figs. 4–8) in a q-range of $0.006 - 0.12$ Å^{-1}. The wavelength of the scattered neutrons registered by the detector was determined according to the time-of-flight method. The calibration procedure was made using vanadium.

Processing of the measured spectrum, calculation of the spectrometer resolution function, data correction carrying out the normalization of the spectrum and subtraction of the background sample data were realized using SAS [10] software program.

2. THEORY

The scattered intensity on an absolute scale for any interacting particulate systems of scatterers can be expressed as [11]

$$I(q) = (\Delta\rho)^2 V_p^2 N_p \langle P(q) \rangle S(q), \tag{1}$$

where $\Delta\rho = \rho_{\rm Fe}, \rho$ is the scattering contrast; and $\rho_{\rm Fe}$ and ρ are the scattering length densities of the Fe particles and polymer matrix, respectively. $\langle \ldots \rangle$ denotes a statistical average and is taken over the available positions and orientations of the particles. V_p is the mean particle volume, N_p is the number of particles per unit volume, $P(q)$ is the scattering form factor for particles given by [2]

$$P(q) = \left| \frac{1}{V_p} \int_{V_p} \mathrm{e}^{i\ \vec{q}\ \vec{r}} d\vec{r} \right|^2 , \tag{2}$$

and $S(q)$ is the structure factor (the inter-particle correlation factor) [2]:

$$S(q) = 1 + 4\pi \frac{N}{V} \int_0^\infty [g(r) - 1] r^2 \frac{\sin(qr)}{qr} dR \tag{3}$$

and is the Fourier transform of the pair distribution function $g(r)$ related to the probability of finding the centre of any particle at a distance R from the center of a given particle. For N particles in a volume V, $(N/V)g(R)dV$ is the number of particles in volume element dV at a distance R from a given particle.

For spherical particles, the form factor from Eq. (2) has the expression [12]:

$$P(q) = \frac{3}{(qR)^3} (\sin(qR) - qR\cos(qR))^2 . \tag{4}$$

The range we are concerned with for determination of specific surface is the so-called Porod regime, where the small-angle scattered component follows a q^{-4} power law whose intensity is proportional to the surface area of the interface between the scattering microstructural phases of interest. In the Porod regime, scattering from the porous material follows the Porod equation [13]:

$$I(q) = \frac{2\pi(\Delta\rho)^2}{q^4} \frac{S}{V} + B, \tag{5}$$

where S/V is the total area of the interface region per unit of volume of the particle and B is the background. Knowing the shape of the particles we are able to determine their dimensions.

3. RESULTS AND DISCUSSIONS

Scattering length density is defined as the ratio of the scattering length per molecule and molecular volume. Having a $X_m Y_n$ molecule, the scattering length density is given by

$$\rho_{X_m Y_n} = \frac{m b_X + n b_Y}{\nu} . \tag{6}$$

Here $m b_X + n b_Y$ is the scattering length per molecule and ν is the volume of molecule $X_m Y_n$ comprising m atoms X and n atoms Y. The molecular volume

ν is given in terms of density d and molar mass m for molecule $X_m Y_n$ and Avogadro number and has the expression:

$$\nu = \frac{m}{N_{\rm av} d}. \tag{7}$$

For Fe particles the density is $d = 7.874\ {\rm g/cm}^3$, the molar mass is $m = 55.85\ {\rm g/mol}$, the scattering length is $b_{\rm Fe} = 9.45 \cdot 10^{-13}$ cm [14], so the molecular volume is $\nu = 1.18 \cdot 10^{-23}\ {\rm cm}^3$ and $\rho_{\rm Fe} = 8.01 \cdot 10^{10}\ {\rm cm}^{-2}$. Proceeding in a similar way, for the polymer matrix $\rho = 0.06 \cdot 10^{10}\ {\rm cm}^{-2}$, so the scattering contrast is $\Delta\rho = 7.95 \cdot 10^{10}\ {\rm cm}^{-2}$.

Figure 4, within the limits of coherent/incoherent scattering, shows the SANS data for Stomaflex creme (lower curve) and Fe particles (upper curve). The scattering intensity for Stomaflex creme reveals a power-law behavior of the form $I(q) \approx q^{-\alpha}$ with the exponent α less than 4. From this value we obtain the fractality dimension of the polymer network. In our case ($\alpha < 4$) the fractal dimension is given by $D_S = 6 - \alpha$ and the polymer matrix exhibits the behavior of a surface fractal object with the fractal dimension $D_S = 2.47 \pm 0.01$, an intermediate value between perfectly smooth surfaces ($D_S = 2$) and surfaces so folded that they almost completely fill the space ($D_S = 3$).

The SANS curve for Fe particles shows also a power-law behavior, but here, on the linear portion of the curve, the slope has a value of 4 showing a sharp interface between the phases. For the low q-values it is seen (Fig. 4) that scattered intensity does not satisfy the Porod law $\approx q^{-4}$ and has higher values

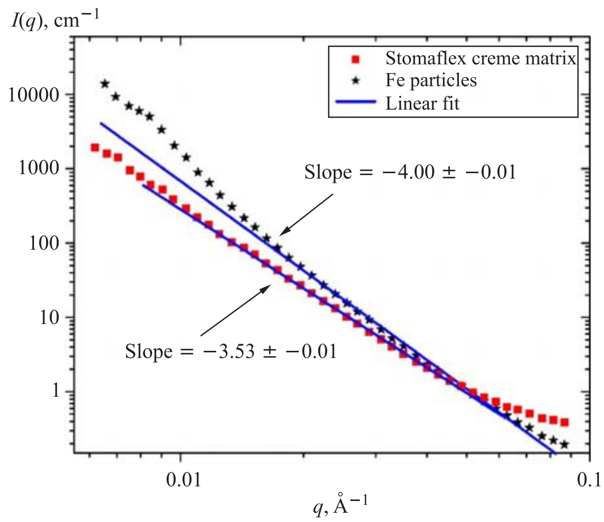

Fig. 4. Experimental curves for Fe particles, polymer matrix and linear fits

due to appearance of the structure factor. This is explained by the formation of aggregates between Fe particles, and deviation from the Porod law is a measure of the interaction of particles inside the aggregates which, as a consequence, shows the presence of this structure factor. We made a fit, in log–log coordinates, for Fe particles (Fig. 4) using the model from Eq. (5). The obtained value for the surface area is $S/V = 0.75 \cdot 10^4\ \mathrm{cm}^{-1}$ and mean value of radius of particle is $R = 2.00 \pm 0.25\ \mu$m, which are in very good agreement with electron microscopy data. Figures 5 and 6 show the SANS data from magnetic elastomers polymerized without and with magnetic field. From Figs. 5 and 6 we can observe that the SANS scattered intensities increase proportionally with increasing the mass concentration of Fe particles inside the magnetic elastomer. Scattering curves for 25, 50 and 75% Fe concentrations can be expressed as an addition (Fig. 5 and Fig. 6) of scattering curves from Fe particles and from polymer matrix (Fig. 4). The profiles of the curves (Fig. 5) have a similar behavior for each concentration showing that in a q-range from 0.006 Å^{-1} up to 0.1 Å^{-1}, the microstructure of magnetic elastomers is the same. A similar effect takes place in magnetic elastomers polymerized in magnetic field (Fig. 6).

The influence of the Fe particles on the scattering from magnetic elastomers is obtained from subtraction of the polymer matrix scattering curve (Fig. 1) and from magnetic elastomer scattering curves (Fig. 5 and Fig. 6) for every concentration.

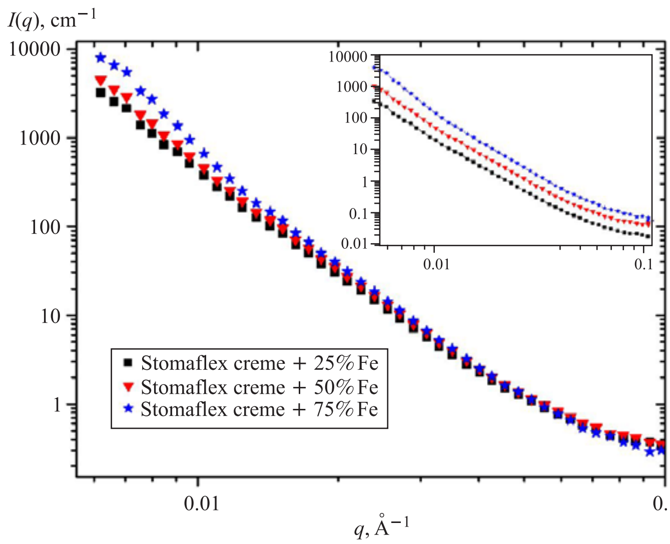

Fig. 5. Experimental curves for magnetic elastomers polymerized in zero magnetic field. Inset graphs show the same curves scaled down by a factor of 2 for 50% Fe and by a factor of 4 for 25% Fe, as compared to curve for 75% Fe concentration

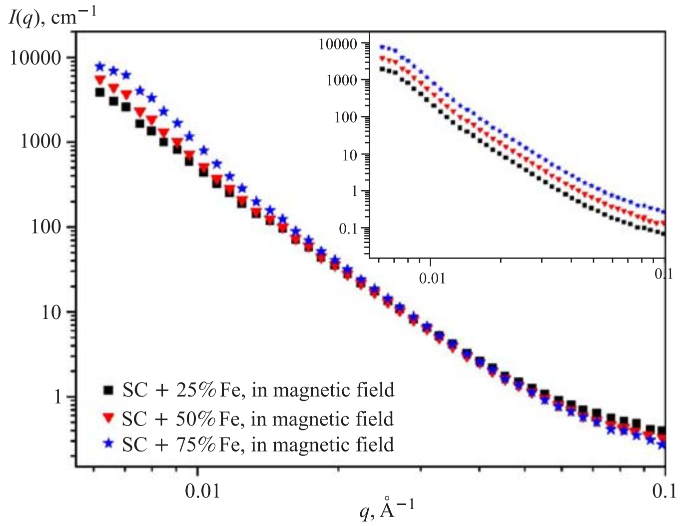

Fig. 6. Experimental curves for magnetic elastomers polymerized in magnetic field, $B = 156.5$ mT. Inset graphs show the same curves scaled down by a factor of 2 for 50% Fe and by a factor of 4 for 25% Fe, as compared to curve for 75% Fe concentration

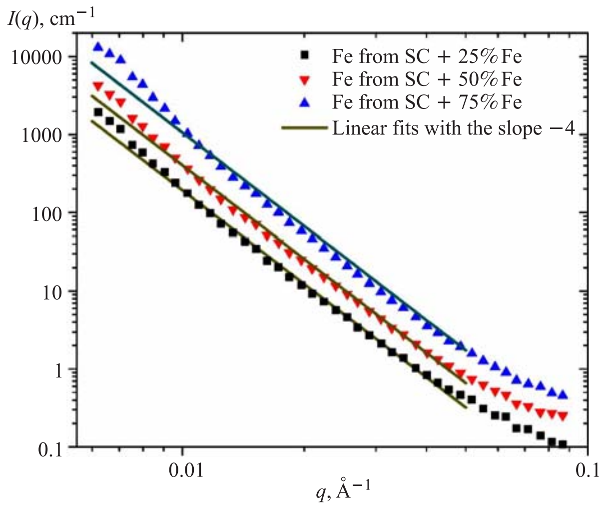

Fig. 7. Scattering curves for magnetic elastomers with various Fe concentrations ($B = 0$, only Fe particles contribution)

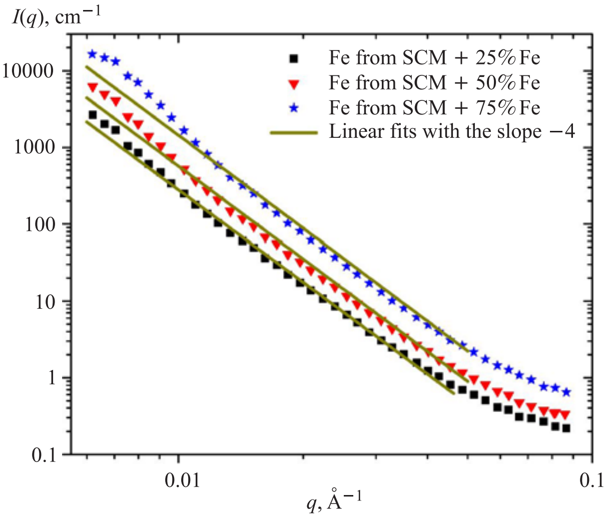

Fig. 8. Scattering curves for magnetic elastomers with various Fe concentrations ($B =$ 156.6 mT, only Fe particles contribution)

The subtraction was carried out taking into account the percent of Fe particles inside the magnetic elastomers. Figures 7 and 8 present the results of this subtraction.

As for pure Fe particles, the scattering from Fe particles inside the elastomer deviates from the Porod law, for low q-values, revealing a homogeneous distribution of aggregates inside the polymer matrix.

The profiles of the curves are the same for each concentration showing that for these sizes of particles, in a q-range of $0.006-0.1$ Å^{-1} and polymerization process in a magnetic field $B = 156.5$ mT the microstructure of magnetic elastomers is the same, the curves being determined by the contribution of the components parts through addition.

CONCLUSION

Electron microscopy images of magnetic elastomers reveal the existence of Fe particles with a mean radius $R = 2.09$ μm and standard deviation $\sigma = 0.26$ μm.

With the Porod law we have determined a mean radius for particles $R = 2.00 \pm 0.25$ μm, in very good agreement with scanning electron microscopy data. The scattered intensity increases proportionally with increasing the mass concentration of Fe particles inside the magnetic elastomer for both types, polymerized with and without magnetic field. Polymer matrix exhibits the behavior of a fractal object with the surface fractal dimension $D_S = 2.47 \pm 0.01$.

The similarities of the scattering curves of Fe particles from magnetic elastomers polymerized without (Fig. 5) and with magnetic field $B = 156.5$ mT (Fig. 6), respectively, are probably due to the partial compensation of low (residual) magnetic moments. The effects associated to a magnetic ordering are possible for q-values much smaller than 0.006 Å^{-1} (which corresponds to dimensions greater than 1000 Å).

Deviations from the Porod law of the scattered intensity from Fe particles are explained by the interaction of particles inside the aggregates. The same deviations appear in scattering from Fe particles after subtracting them from Stomaflex creme polymerized with and without magnetic field, respectively.

Dependence of the specific surface behavior on the size of particles in such systems is in our plan for future investigations.

Acknowledgments. E. M. Anitas gratefully acknowledges the help of Dr. A. Kh. Islamov and Dr. M. L. Crauss for many useful discussions, the support from the grant No. 3805-3-07/08 of the Romanian Governmental Representative at JINR and the support from the theme 01-3-1030-99/2008 of JINR.

REFERENCES

1. *Brandrup J., Immergut E. H., Grulke E. A.* Polymer Handbook. 4th ed. Wiley-Interscience, 1999.

2. *Lindner P., Zemb Th.* Neutron, X-Rays and Light Scattering: Scattering Methods Applied to Soft Condensed Matter. North-Holland, 2002.

3. *Higgins J. S., Benoit H. C.* Polymers and Neutron Scattering in Condensed Matter. Clarendon Press, 1994.

4. *Roe R. J.* Methods of X-Rays and Neutron Scattering in Polymer Science. Oxford University Press, 2000.

5. *Feigin L. A., Svergun D. I.* Structure Analysis by Small-Angle X-Ray and Neutron Scattering. N.Y.: Plenum Press, 1987.

6. *Bica I.* // Mater. Sci. Eng. B. 2003. V. 98. P. 89–93.

7. http://www.mcid.co.uk

8. *Ostanevich Yu. M.* // Makromol. Chem. Macromol. Symp. 1998. V. 15. P. 91–103.

9. *Kuklin A. I., Islamov A. Kh., Gordeliy V. I.* // Neutron News. 2005. V. 16, No. 3. P. 16–18.

10. *Soloviev A. G., Solovieva T. M., Stadnik A. V., Islamov A. Kh., Kuklin A. I.* JINR Preprint P10-2003-86. Dubna, 2003.

11. *Hansen J. P., McDonald J. A.* Theory of Simple Liquids. 3rd ed. Academic Press, 2006.

12. *Guinier A., Fournet G.* Small-Angle Scattering of X-Rays. N.Y.: John Wiley and Sons, 1955.

13. *Porod G.* X-Ray Small-Angle Scattering of Close-Packed Colloid Systems: I // Kolloid Z. 1951. V. 124. P. 83.

14. *Sears V. F.* // Neutron News. 1992. V. 3. P. 29–37.

Received on October 16, 2008.

Корректор *Т. Е. Попеко*

Подписано в печать 8.12.2008.
Формат $60 \times 90/16$. Бумага офсетная. Печать офсетная.
Усл. печ. л. 0,93. Уч.-изд. л. 1,32. Тираж 305 экз. Заказ № 56449.

Издательский отдел Объединенного института ядерных исследований
141980, г. Дубна, Московская обл., ул. Жолио-Кюри, 6.
E-mail: publish@jinr.ru
www.jinr.ru/publish/